Int. J. Electrochem. Sci., 9 **(2014)** 1250 - 1263

International Journal of
ELECTROCHEMICAL
SCIENCE
www.electrochemsci.org

Mathematical Modeling for Hard Trivalent Chromium Coatings Thickness with Thin Zincates Interlayer on Pure Aluminum

E. Khodadad[*], *M.K. Lei***

Surface Engineering Laboratory, School of Materials Science and Engineering, Dalian University of Technology, Dalian 116024, China
[*]E-mail: khodadaderfan@mail.dlut.edu.cn
**E-mail: surfeng@dlut.edu.cn, mklei@dlut.edu.cn

Received: 31 October 2013 / *Accepted:* 11 December 2013 / *Published:* 5 January 2014

The trivalent chromium coatings were deposited on the pure aluminum substrate using a thin zincates interlayer. Zincates has considerably influenced in the formation of trivalent chromium deposit on the pure aluminum substrate. The plating temperatures, plating times and different pH ranges had significant effects on the thickness, uniformity and microstructure of trivalent chromium plating on the pure aluminum substrate. Results show the average thickness for homogenous chromium coating without pitting and microcracks was 35 μm at 30° C, pH = 2 and 40 min. The Vickers microhardness of the chromium coating was about HV 8.3 GPa under a load of 1 N. Experimental results were mathematically modeled with the response surface methodology (RSM) method by statistical software SPSS 19 and Design expert V6 to predicted coating thickness at different coating conditions.

Keywords: Aluminum substrate; trivalent chromium electroplating; zincates interlayer; mathematical modeling; RSM

1. INTRODUCTION

After steel and ferrous alloys, aluminum constitutes the largest group of materials widely used in advanced industries such as aerospace and automobile. However, aluminum shows low mechanical properties such as hardness and wearing resistance [1, 2]. Considerable research on increasing the mechanical properties of aluminum using electroless nickel plating has been previously carried out [3-6]. Chromium plating can be a good alternative replacement, as it has better morphology and surface quality compare to nickel electroplating [7]. Chromium plating is the most widely used for electroplated on copper and stainless steel substrate to obtain high quality of surface properties [8-12]. Zeng et al. [10] shows trivalent chromium coating with crack-free structure has good corrosion properties. Protsenko et al. [13] showed some wetting agents should be used in order to achieve fine crack-free structure in trivalent chromium coating. Li et al. [9] expressed the current densities have important influence on the coating microstructure and composition. Glossy and crack-free deposited coatings which have good corrosion properties could be obtained under lower current densities. Successful electroplating of trivalent chromium may impart good mechanical properties such as hardness, wear, and abrasion resistance to aluminum substrates.

Electroplating of trivalent chromium directly on the aluminum substrate has not become commercially successful due to formation of the oxide films on the aluminum surface, which inhibit the direct electroplating of chromium coating on the pure aluminum [2]. Since aluminum exposed to air is always covered by a dense oxide coating, that must be removed before the parts can be plated, otherwise applied the chromium coating will be prevented. As regards aluminum has high potential reactivity with trivalent chromium solutions. Trivalent chromium bath are so acidic and chrome ions on the electromotive scale being very attracted to the pure aluminum substrate. It may cause prevent the successful deposition of the trivalent chromium coating on the pure aluminum substrate. Preparation of aluminum surface is quite specific, to protect re-oxidation of the aluminum surfaces during processing, zinc immersion deposits “zincates” are used for electroless nickel plating [14-17]. Previous research on electroless nickel coating on aluminum substrates showed that the zincates interlayer has considerably influence on the formation of deposits [3-5]. One of the steps proceeding for electroplating of trivalent chromium on the pure aluminum is the process of zincate immersion. The application of this process allows considerable improvement of the adhesion of the trivalent chromium to the aluminum substrate. The zincate protects aluminum against re-oxidation from atmospheric exposure. However zincates have very active redox reactions with trivalent chromium ions. Furthermore, the deoxidized parts must be protected during the transfer, to avoid re-oxidation of the highly active aluminum surfaces. In this study effect of the zincates interlayer on the direct deposition of trivalent chromium on pure aluminum substrates instead of other interlayer such as copper and nickel was studied. Commonly, chromium coatings are deposited from hazardous hexavalent chromium baths. In view of a very high toxicity of hexavalent chromium compounds, development of chromium electroplating processes on the base of trivalent chromium salts is a very important task of modern electroplating. Research on electroplating of trivalent chromium on pure aluminum substrate still devisable and was not adequate.

The mathematical modeling is one of the unique subjects in modern electrochemistry. In the terms of mathematic modeling refers to a process of determining an appropriate description of reality that approximates its behavior to some specified degree of accuracy. Models are constructed using well-understood primitive components, or building blocks, defined by their inherent functionality and also their interaction mechanism, typically the manner by which data are communicated among them. A model is often most useful when it fails to fit the data, because that says that some of the ideas about the study system are wrong. In this research experimental result was mathematically modeled by response surface methodology (RSM) with statistical mathematics modeling to predict the properties of hard trivalent chromium coatings. Previously response surface methodology (RSM) was used to improve electroplating of Au-Sn alloys and coefficient of friction and mechanical behavior of fiber-reinforced polymeric composite composites [18, 19]. The present model was prepared with statistical software SPSS 19 and Design-expert V6. Linear and polynomials were fitted to the experimental data to obtain the regression equations. This model can be used to predict thickness of the trivalent chromium coatings with the same chemical composition and deposition conditions.

2. EXPERIMENTAL SECTION

Pure commercial aluminum plates with an area of 6 cm^2 were used as substrates. Dimensionally stable titanium anodes (MMO) commercially obtained from Xinxiang Future hydrochemistry Co., China, with an area of 12 cm^2 was used in order to reduce the anodic oxidation of Cr (III). Before plating, the substrates were polished and activated in HNO_3 solution with a concentration of 50 vol.% for 15 s. Finally, the substrates were washed in alkaline solution and dried in the air atmosphere. Zincates were deposited from bath Sodium hydroxide (525 g/l), Zinc oxide (100 g/l), Ferric chloride (1 g/l) and Potassium sodium tartrate (10 g/l) at room temperature. Electroplating of trivalent chromium as deposited from baths composed of $CrCl_3 \cdot 6H_2O$ (200 g/l), HCOOH (32 ml/l), CH_3COOH (10 ml/l), NH_4Cl (30 g/l), KCl (60 g/l), H_3BO_3 (30 g/l). Trivalent chromium was deposited at a steady value of current density (30 A/dm^2) and the pH range from (1.5-2.5) and the experiment for investigated better morphology and roughness and enough thickness were run in different temperatures from 25-35° C and time 20-60 min. Chromium electroplating was carried out in a usual thermo stated glass cell. In order to provide formation of stable Cr^{+3} ions complexes, a thermal treatment of the chromium bath was performed at a room temperature for 24 h. The current efficiency of chromium electroplating was calculated by comparing the weight gain of the cathode placed in the chromium plating bath [20]. The average values of current efficiency as well as chromium electroplating rate were calculated for each bath solution on different coating conditions.

The surface morphology and composition of the coating were investigated by a Carl Zeiss NTS GMBH–SUPRA55-32-76 scanning electron microscopy (FE-SEM). Cross-sectional composition of the coating was measured by an EPMA1600-SHIMADZU electron probe micro-analysis (EPMA). The coating hardness was characterized by Vickers microhardness (HV) using a HXD-1000TM tester under a 1 N load.

3. RESULTS AND DISCUSSION

3.1. Pretreatment of Al substrate and Zincates interlayer

Pure aluminum is quite active, redox reactions during zincates coating and thermodynamic reactions occur during trivalent chromium coating respectively. Zincates are an electrochemical exchange reaction between zinc complexes in solution and the aluminum substrate, depositing zinc crystallites at the expense of aluminum dissolution. The zincates protect the Al substrate, effectively providing a sound basis for subsequent deposition. During the zincates process the aluminum oxide film is first dissolved in zincates solution as follows Eq. 1 [3]:

$$Al_2O_3 + 2NaOH + 3H_2O \rightarrow 2NaAl(OH)_4 \quad (1)$$

Considering a specific system, the exchange process occurring during the zincate treatment of Al can be represented by the following Eq. 2 [1].

$$3Na_2(ZnOH)_4 + 2Al_{(substrate)} \rightarrow 2NaAl(OH)_4 + 4NaOH + 3Zn_{(deposited)} \quad (2)$$

Reaction in solution of Cr (III) before ions reach thermodynamic equilibrium state aqueous ammonia (alkaline) green color Cr (III) hydroxide is precipitated, Eq. 3 [21].

$$[Cr(H_2O)_6]^{3+}_{(aq)} + 3OH^-_{(aq)} \rightarrow [Cr(OH)_3(H_2O)_3]_{(s)} + 3H_2O_{(l)} \quad (3)$$

The hydroxide readily dissolves in acids to form salts, after ions reach thermodynamic equilibrium, dark blue color chromium ions is precipitated, Eq. 4.

$$[Cr\,(OH)_3(H_2O)_3]_{(s)} + 3H_3O^+_{(aq)} \rightarrow [Cr(H_2O)_6]^{3+}_{(aq)} + 3H_2O_{(l)} \quad (4)$$

The redox equations reactions between reactions (2) and (3) will happen on the surface of the zincates are, Eq. 5. Upon completion of reaction (5) the zincates will be removed, in this case the reduction of Cr^{+3} to Cr should start before Eq. 5 in the electrochemistry cell up to chromium coating will be deposited on the aluminum surface uniformly:

$$2Cr^{3+}_{(aq)} + Zn_{(s)} \rightarrow 2Cr^{2+}_{(aq)} + Zn^{2+}_{(aq)} \quad (5)$$

If this process continued after short time zincate will be removed and pure Al will appear in surface. Cr (III) has a redox reaction, with aluminum, Eq. 6 [22]:

$$Cr^{3+} + 2Al_{(s)} \rightarrow Al_2O_{3(s)} + 2Cr \quad (6)$$

The trivalent chromium baths was so acidic and Cr^{+3} ions were very positive to the aluminum surface on the electromotive scale and aluminum oxide would forms and it lead to prevent sufficient adhesion of the chromium coating on the aluminum surface. Burzynska et al. [4] found after 4 min, the zincates thickness will be stable. For increasing the zincates layer, this process was executed four times.

Figs. 1 and 2 show EPMA results of map and line scanning of element distribution to investigated cross-sectional examination of the trivalent chromium coating. Result shows the zincate was very thin. However it prevents the oxidation of the aluminum surface and provides the opportunity for the formation of chromium coating.

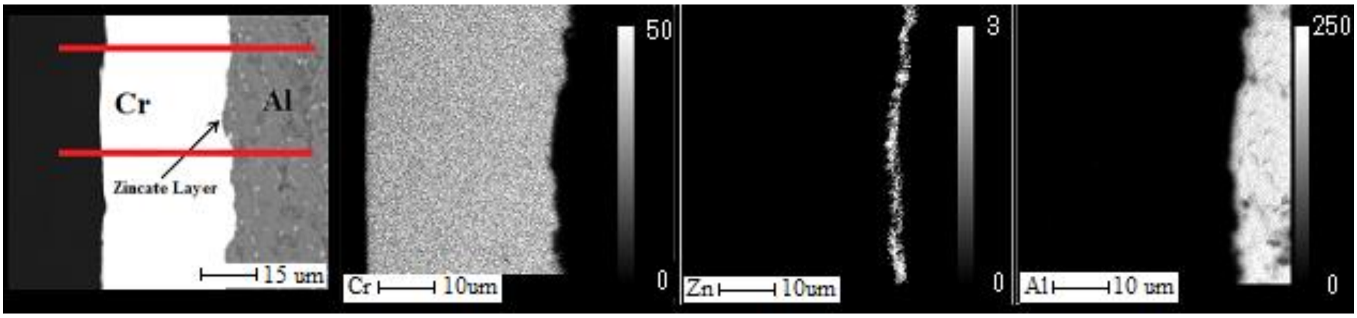

Figure 1. EPMA data: Map cross view scanning of element distribution of the coating, at 30° C, plating time was 40 min, and pH=2.

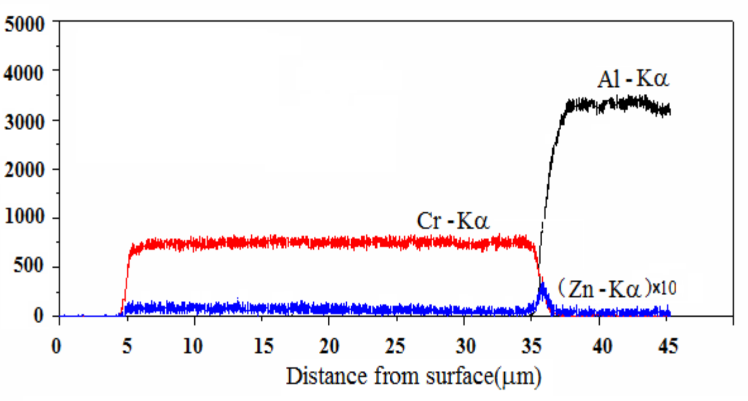

Figure 2. EPMA data: Line scanning of element distribution of the coating, at 30° C, plating time was 40 min, and pH=2.

3.2. Current efficiency

Fig. 3 shows effects of the different plating temperatures, plating times and pH ranging on current efficiency of chromium coating for different samples. The current efficiency of chromium electroplating was calculated by comparing the weight gain of the cathode placed in the coating process. Current efficiency (η %) was calculated as the ratio between the experimental and theoretical weight uptakes as described in a previous work [23]: $\eta\% = (\Delta W_{meas}/\Delta W_{theo}) \times 100\%$. Previous research shows a current efficiency for trivalent chromium was near 30-35% [24-26]. The current efficiency of chromium electroplating for trivalent chromium bath was sufficiently greater than in the case of ordinary hexavalent chromium baths [25]. It should be stressed that the current efficiency of traditional chromium baths with simple solution without any special buffering does not exceed 10-20% [24]. However, in this study the current efficiency is near 29% at 30° C and 30 A/dm^2. Nevertheless in comparison to high toxic hexavalent chromium bath, current efficiency still was higher. However these results shows current efficiency was lower than previous studied for trivalent chromium coatings [8, 10, 27]. It is believed the reaction between chromium ions and zincates layer which results in the disappearance of a number of trivalent chromium ions. The zincates after sample doped inside of the bath were dissolved on the solution and were reacted to Cr^{3+} ions in the start of the coating process. The result of this reaction possibly was Cr^{3+} to Cr^{2+} and Zn to Zn^{2+}. Reduction of complex Cr^{+2} to the Cr need charging more energy and possibly it is the reason why the current efficiency was lower for this process. The rate of electroplating reaction was controlled by the diffusion of the complex Cr^{3+} ion to the cathode surface. Therewith the rate of chromium deposition was stated to be decreased rapidly with deposition time after 10 minutes [26]. The principal problem seems to be formation of Cr (III) hydroxo-complexes in the near-electrode layer during Cr-deposition. The electrode surface may be blocked by poorly soluble adsorbed hydroxide compounds of Cr^{3+} [28]. Therefore, the rate of chromium plating diminishes. In addition, the particles of the Cr^{3+} hydroxide solution are incorporated into coating structure, which causes cracking, and darkening of deposits and decreasing the current efficiency.

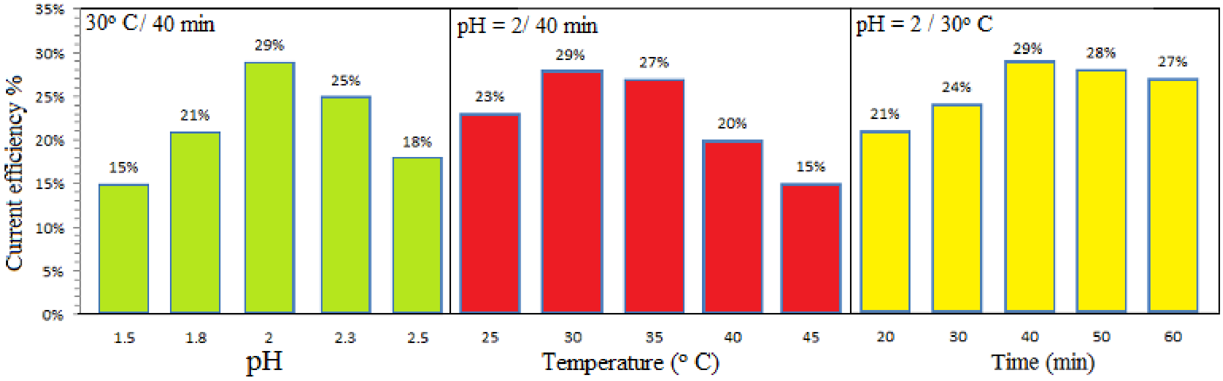

Figure 3. Dependencies of current efficiency upon the different pH ranges (1.5-2.5), plating temperatures (25-35° C) and plating times (20-60 min) for trivalent chromium coatings at 30 A/dm^2.

3.3. Microstructure and morphology

Fig. 4 shows the SEM observation of trivalent chromium coating in different plating temperature, plating times and pH ranging. Fig. 4 (a-c) shows the effect of different temperatures ranging from 25 to 35° C at pH = 2 with 40 min plating time. Fig. 4 (d-f) shows these effects for plating times ranging from 20-60 min at pH = 2 and 30° C. Similarly fig. 4 (g-i) shows effect of different pH ranging from 1.5-2.5 at 30° C and 40 min on the deposition of trivalent chromium coating at 30A/dm^2. Fig. 2 (a-c) shows at 25° C, the morphology of the coating shows micro-porous and pitting surface, However at 30° C the coatings morphology was smooth, uniform and without major pitting. At 35° C the surface roughness was increased and some micro-pitting was observed in the vicinity of large chromium grains. This results was expressed the best temperature for chromium coatings was at 30° C. The effect of the temperature is very typical and salient on the morphology and structure of the trivalent chromium coatings on the pure aluminum substrate with thin zincates interlayer. The author suggests this occurs, because of the reaction between zincates interlayer and trivalent chromium bath and therewith edge effecting occurs at the same time. Commonly the current density is higher at the edges than center of the cathode [29]. This is because the current flow passes partially around the rectangular space between the electrodes. However because of increasing current density at the edges of the samples can be easily noticed by observing the quality of the chromium electroplating. In some cases the deposit in the central part of the cathode may be compact and flat whereas the occurrence of dendrites is observed at the edges and contrary micro-porous structure. The appearance of dendrites at the edges of the samples also in such situations was one of the problems related to the current density distribution, because the growing dendrites could cause short circuits followed by a decrease in the current efficiency, or even damage the power supply [30]. Fig. 4 (d-f) shows with increasing the plating time the coating morphology was slightly changed and the size of the chromium grains on the surface was slightly increased. However the current efficiency with increasing the plating time was decreased strongly. It may because the rate of chromium deposition was stated to be decreased rapidly with deposition time after 10 minutes [27]. This results was expressed the best plating time with highest current efficiency for trivalent chromium coating on the pure aluminum substrate was at 40 min and 30° C. Fig. 4 (g-i) shows the effect of different pH ranging on the morphology of the trivalent chromium coatings. These results expressed with increasing the pH up 2 the deposition rate and current efficiency was increased extremely, However when pH was more than 2 the coating roughness was increased and the microcracks and pitting was formed on the coatings surface.

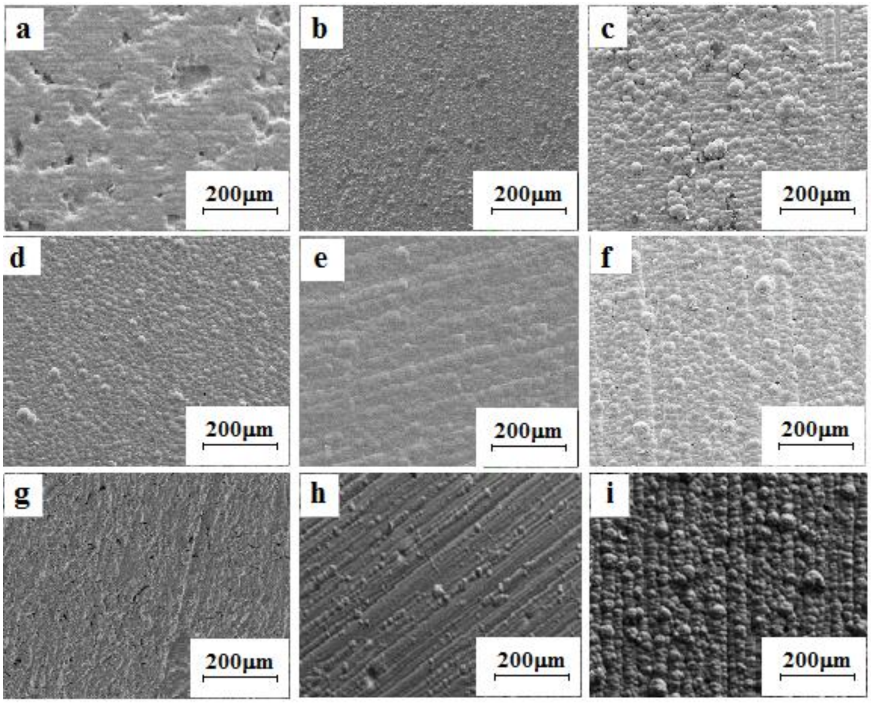

Figure 4. Effects of different temperatures ranging (a-c) from 25 to 35° C at pH=2 with 40 min plating time. Effects of different plating times ranging (d-f) from 20-60 min at pH=2 and 30° C. Effect of different pH ranging (g-i) from 1.5-2.5 at 30° C and 40 min on the deposition of trivalent chromium coating at 30A/dm^2.

3.4. *Mathematical Modeling for Trivalent Chromium Thickness*

Table 1. Primary coatings input variables for experimental design levels for mathematical modeling of trivalent chromium coatings, at 30 A/dm^2.

Variables	-1	0	1
Temperature (^{o} C)	25	30	35
Time (min)	20	40	60
pH	1.5	2	2.5

Mathematical model was based on a three level Box–Behnken [31] design with full replication. Temperature (T_c), plating time (t_c) and pH was used as coatings independent input variables. Table 1 show coatings input variables and experimental design levels used. RSM was applied to the experimental data using statistical software, Design-expert V6. Linear and polynomials were fitted to the experimental data to obtain the regression equations. The sequential F-test, lack-of-fit test and other adequacy measures were used in selecting the best models.

The design matrix and the average measured responses were calculated by statistical software. Estimation of a full quadratic model with the general description: $N = 2^{k-p} + 2k + C_o$, [32] where (N) is the number of experiments, (k) is the number of independent variables, (p) the fractionalization number and C_o is the number of central points, required for curvature estimation. To investigate the primary parameters the initial experimental set up was prepared. Table 2 shows the initial parameters for investigating thickness of trivalent chromium coatings in this research.

Table 2. Initial coatings parameters input for experimental design levels for mathematical modeling of trivalent chromium coatings, at 30 A/dm^2.

Std.	RUN	Factor 1- Temperature	Factor 2 - Time	Factor 3 - pH
9	1	0.00	-1.00	-1.00
4	2	1.00	1.00	0.00
8	3	1.00	0.00	1.00
3	4	-1.00	1.00	0.00
5	5	-1.00	0.00	-1.00
10	6	0.00	1.00	-1.00
14	7	0.00	0.00	0.00
15	8	0.00	0.00	0.00
11	9	0.00	-1.00	1.00
7	10	-1.00	0.00	1.00
16	11	0.00	0.00	0.00
12	12	0.00	1.00	1.00
17	13	0.00	0.00	0.00
2	14	1.00	-1.00	0.00
6	15	1.00	0.00	-1.00
1	16	-1.00	-1.00	0.00
13	17	0.00	0.00	0.00

Fig. 5 shows the effect of the different plating temperatures (a), plating times (b) and pH (c) ranging on the coating thickness of chromium coating for different samples. It was before stated that it is not easy to obtain thick deposits from trivalent chromium baths and the rate of chromium deposition was stated to be decreased rapidly with deposition time, and after 10 minutes. Fig. 5 (a) shows the thickness of the chromium coating at pH = 2 and plating time was 40 min. The coatings thickness was decreased when the plating temperature was more than 34-36° C. It is believed that with increasing the plating temperature, the speed of reaction between zincates interlayer and chromium ions also was increased and it was leads to the ultimate the collapse and lack of proper adhesion of the trivalent chromium coating to the aluminum substrate in the start of the coating process. Fig. 5 (b) shows the thickness of the chromium coating at 30° C and pH=2. Results show the coating thickness after 40 min was constant and increased very slightly; it may because of the formation of Cr^{+3} hydroxo-complexes near the anode during chromium deposition. Fig. 5 (c) shows the effects of the pH on the thickness of the trivalent chromium coating.

Commonly in the normal bath containing formic acid, the drop of hydrogen gas current efficiency from 100% at -1.06 V versus SHE corresponds to the beginning of trivalent chromium ion reduction. Hydrogen evolution is the most dominant reaction during the trivalent chromium plating process [20]. Most of the electricity passed through the cell was consumed by the hydrogen evolution reaction, which increases the pH of the solution at the cathode surface especially at high cathode over potentials. The sequence of electroplating of chromium involved the reduction of a complex Cr^{3+} ion to a complex Cr^{2+} ion and then from the complex Cr^{2+} ion to $Cr_{(s)}$. The rate of electroplating reaction was controlled by the diffusion of the complex Cr^{3+} ion to the cathode surface [20]. When the pH is higher than 2, the rate of evaluation of the hydrogen also is higher and it had worst effect on the surface roughness and leads to the lower rate of the trivalent chromium ions reduction to the chromium coating.

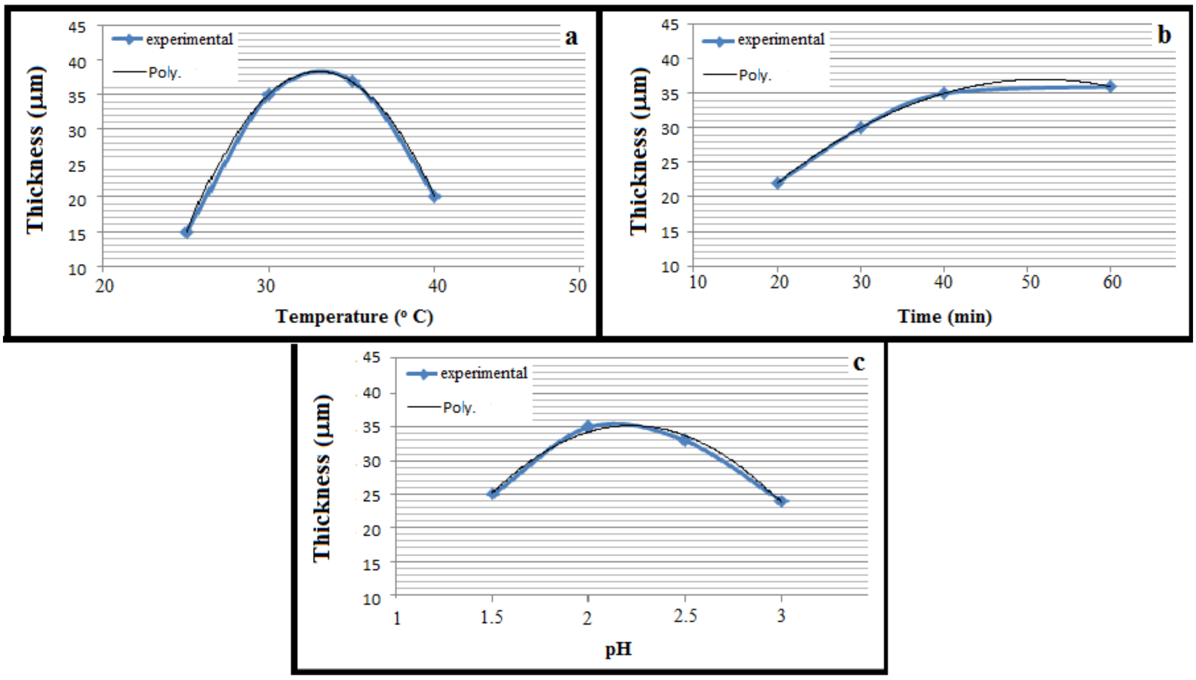

Figure 5. Effects of the different plating temperatures (a) at (pH = 2, plating time = 40 min), plating times (b) at (Temperature = 30° C, pH=2) and different pH (c) ranging at (Temperature =30° C, plating time = 40 min) on the coating thickness of chromium coating for different samples at $30 A/dm^2$.

A stepwise regression method was used to fit the second order polynomial Eq.7 to the experimental data and to identify the relevant model terms. The same statistical software was used to generate the statistical and response plots. The response function of coating thickness dimensions can be expressed by Y=f (T_c, t_c and pH) for trivalent chromium coatings [33].

$$Y_{Thickness} = b_0 + \sum_{i=1}^{4} b_i x_i + \sum_{i=1}^{4} b_{ii} x_i^2 + \sum_{\substack{i=1 \\ i<j}}^{4} b_{ij} x_i x_j \qquad (7)$$

Where b_o is constant of the regression equation, coefficients b_1, b_2, b_3, are linear terms, the coefficients b_{11}, b_{22}, b_{33}, are quadratic terms and the coefficients b_{12}, b_{13} and b_{23} are interaction terms. Analyzing was measured responses by the design expert software. The fit summary output indicates that the RSM model is statistically significant for the coating thickness ‘the second response’ therefore it will be used for further analysis. While for the other responses the quadratic models are statistical recommended for further analysis. The final mathematical models in terms of actual factors as determined by statistic software SPSS 19 are shown in Eq.8 for the prediction of coating thickness ($Y_{Thickness}$) for trivalent chromium coatings.

$Y_{\text{Thickness (µm)}} = -0.12117 \times (T_c)^2 - 6.12656E{-}003 \times (t_c)^2 - 4.99750 \times (pH)^2 + 0.000001 \times (T_c \times t_c) + 0.10050 \times (T_c \times pH) + 0.025000 \times (t_c \times pH) + 7.78437 \times (T_c) + 0.56237 \times (t_c) + 19.83375 \times (pH) - 130.34375$

The test for significance of the regression models and the lack-of-fit test were performed using the same statistical package. By selecting the step-wise regression method, which eliminates the insignificant model terms automatically, the resulting ANOVA Tables 3 for the reduced quadratic models summarize the analysis of variance of each response and show the significant model terms. The table show the adequacy measures R-Squared=0.9990, Adj R-Squared=0.9981, Pred R-Squared=0.9903, Adeq Precision=100.628and F-value of 1026.62 implies the model is significant. Values of "Prob > F" less than 0.0500 indicate model terms are also significant. In this research "Prob > F" T_c, t_c and pH values are significant in model terms. Values greater than 0.1000 indicate the model terms are not significant. The entire R-Squared measures are close to 1, which is in reasonable agreement and indicate adequate models. The adequate precision ratio above 4 indicates adequate model discrimination in this experiment it 100.628. The analysis of variance indicates that for the coating thickness ($Y_{Thickness}$), the main effect of the temperature (T_c), plating times (t_c), the two level interaction of coating conditions ($T_c \times t_c$), ($T_c \times pH$), ($t_c \times pH$) are the most significant associated terms model for ($Y_{Thickness}$).

Table 3. ANOVA for response surface quadratic model for trivalent chromium coating at 30 A/dm^2.

Source	Sum of Squares	df	Mean Square	F Value	p-value Prob > F
Model	257.95	8	32.24	1026.62	< 0.0001
T_c - Temperature	*39.53*	1	39.53	1258.57	< 0.0001
t_c -Time	*15.96*	1	15.96	508.26	< 0.0001
pH	*3.88*	1	3.88	123.64	< 0.0001
($T_c \times pH$)	*0.25*	1	0.25	8.04	0.0220
($t_c \times pH$)	*0.25*	1	0.25	7.96	0.0224
T_c^2	*38.64*	1	38.64	1230.31	< 0.0001
t_c^2	*25.29*	1	25.29	805.12	< 0.0001
pH^2	*6.57*	1	6.57	209.26	< 0.0001
Residual	0.25	8	0.031		
Lack of Fit	*0.25*	4	0.063		
Pure Error	*0.000*	4	0.000		
Cor. Total	258.20	16			

*Significant Model, R-Squared=0.9990, Adj R-Squared=0.9981, Pred R-Squared=0.9903, Adeq Precision=100.628

Fig.6 indicated that the developed models are adequate because the residuals in prediction of each response are optimal, since the residuals tend to be close to the diagonal line. The present model analysis indicated that there is a polynomial relationship between the effects of the three parameters.

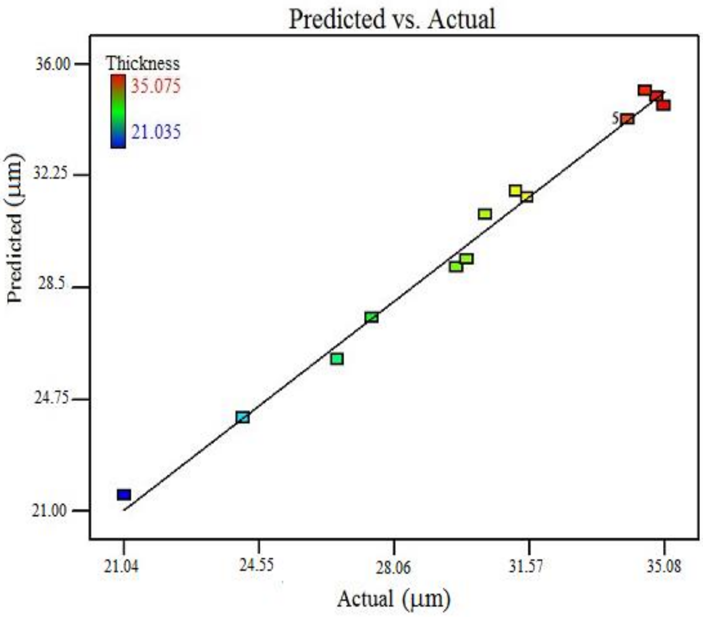

Figure 6. Scatter diagram for (Predicted vs. Actual) of the developed mathematics model for trivalent chromium coating thickness at 30 A/dm^2.

Fig.7 (a,b) shows the effect of (T_c and t_c) on the coating thickness and the contour graph of the (T_c and t_c) effects on the coating thickness at 30 A/dm^2 and pH = 2. Results show that the plating times and plating temperatures are significantly affecting on the coating thickness.

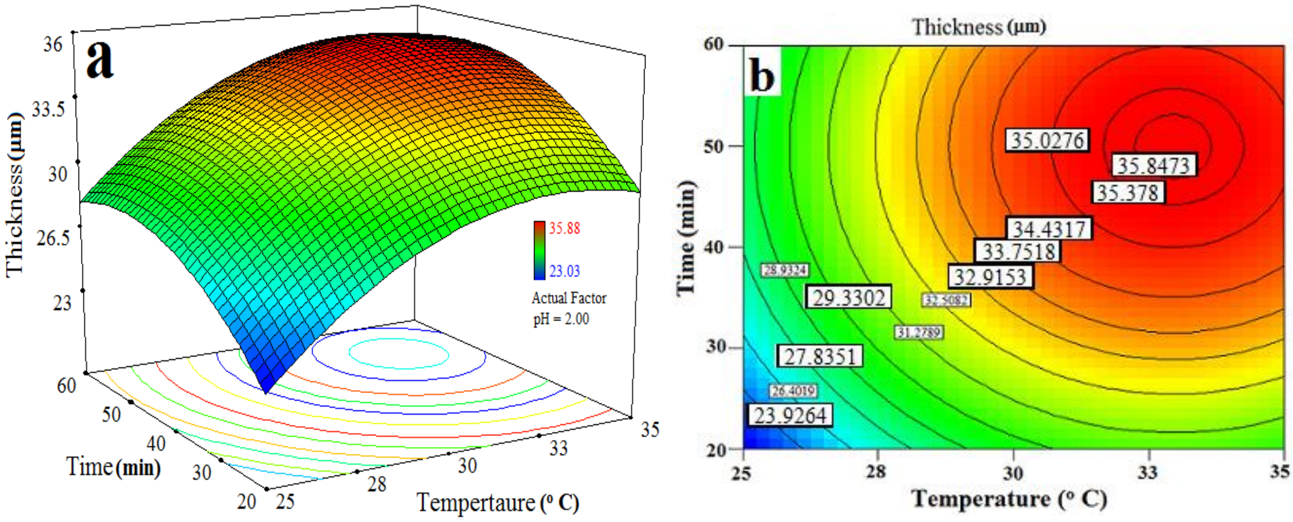

Figure 7. (a) 3D graph shows the effect of (T_c) and (t_c) on trivalent chromium coating thickness and (b) Contour graph shows the effect of (t_c) and (T_c) on the trivalent chromium coating thickness at pH=2, 30A/dm^2.

To better understanding of the mathematics model, the chromium coatings was prepared at 32° C, pH = 2 for 45 min to investigated coating properties. Fig. 8 shows thickness of this trivalent chromium coating. The average of experimental coating thickness was 35.26 μm and the mathematics model predicted this value 35.573 μm. SEM observation shows the adhesion of the coatings were satisfactory and the model which is in reasonable agreement to experimental data. Fig. 10 shows x-ray diffraction spectra of chromium layers prepared in trivalent chromium baths. Result shows the chromium coating has the amorphous type microstructure. The Vickers microhardness at 1 N load was measured HV 8.3 GPa.

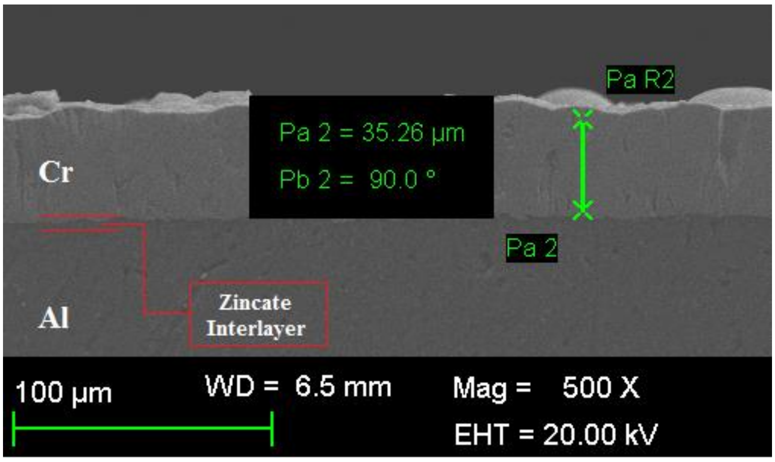

Figure 8. Cross sectional view of the chromium coatings was prepared at 32° C, pH = 2 for 45 min to investigated mathematics model vs. experimental data.

4. CONCLUSIONS

The trivalent chromium coatings were deposited on the pure aluminum substrate using a thin zincates interlayer. Zincates has considerably influence on the formation of trivalent chromium deposit on the pure aluminum substrate. Preventing reaction between the zincates, aluminum surface and chromium ions, is very difficult. Three main coating parameters (T_c, t_c, pH) considerably have effects on the morphology and microstructure of the trivalent chromium coating. However by controlling the temperature the edge effecting and deposition rate will change impressive, which causes it is possible to achieve an appropriate coating. With increasing the temperature from 25° C to 35° C rate of the reaction between zincate and chromium ions will increase also simultaneously the rate of deposition was appropriate. Obtain thick deposits from trivalent chromium baths was not easy and the rate of chromium deposition was stated to be decreased rapidly with deposition time, and after 10 minutes. The optimized plating conditions to obtain the thick coatings (≈ 35μm) was at 30 A/dm^2, 30° C and pH = 2 for 40 min. Chromium coating was amorphous and hardness was HV 8.3 GPa. The maximum current efficiency was achieved as 29% at optimal condition. Commonly, electroplating of hard chromium coatings are deposited from hazardous hexavalent chromium baths. In view of a very high toxicity of hexavalent chromium compounds, development of chromium electroplating processes on the base of trivalent chromium salts is a very important task of modern electroplating. Recently in Europe use the maximum concentration in liquid effluent should be less than ~0.1 μgL^{-1}. In this research experimental results will be mathematically modeled by Response Surface Methodology (RSM) with statistical mathematics modeling to predict the properties of hard chromium coatings. The linear and polynomials will be fitted to the experimental data to obtain the regression equations. Box–Behnken design can be employed to develop mathematical models. Response surface methodology (RSM) was designed to predict the thickness of the trivalent chromium coating. The desired high quality thick trivalent chromium coatings can be achieved by choosing the working condition used in this developed models.

ACKNOWLEDGEMENT
We acknowledge contributory discussions and technical assistant of W. Zhang, C. J. Sun, and S. Tong in this research. One author (Erfan Khodadad) gratefully acknowledges Chinese Scholarship Council (CSC), China, for the financial support.

References

1. E. Stoyanova and D. Stoychev, *J. App. Electrochem.*, 27 (1997) 685.
2. W. Deqing, S. Ziyuan , and K. Tangshan, *Surf. Coat. Technol.*, 191 (2005) 324.
3. E. Khan, C. Oduoza , and T. Pearson, *J. App. Electrochem.*, 37 (2007) 1375.
4. L. Burzyńska, E. Rudnik , and K. Ćwięka, *Archives Met. Mat.*, 54 (2009) 845.
5. M. Hino, K. Murakami, Y. Mitooka et al., *Mat.Trans.*, 50 (2009) 2235.
6. K. Murakami, M. Hino, R. Furukawa et al., *Mat.Trans.*, 51 (2010) 78.
7. W. h. Hui, J. j. Liu, Y. s. Chaug et al., *Wear*, 192 (1996) 165.
8. S. Kwon, M. Kim, S. Park et al., *Surf. Coat. Technol.*, 183 (2004) 151.
9. B. Li, A. Lin , and F. Gan, *Surf. Coat. Technol.*, 201 (2006) 2578.
10. Z. Zeng, A. Liang , and J. Zhang, *Electrochim. acta.*, 53 (2008) 7344.
11. F. Danilov, V. Protsenko, T. Butyrina et al., *Prot. Met. Phys. Chem. Surf.*, 47 (2011) 598.
12. R. Giovanardi and G. Orlando, *Surf. Coat. Technol.*, 205 (2011) 3947.
13. F. Danilov, V. Protsenko, V. Gordiienko et al., *App. Surf. Sci.*, 257 (2011) 8048.
14. A. H. Du Rose Chromium Nickel Plating: Google Patents (1971).
15. B. S. Xu, H. D. Wang, S. Y. Dong et al., *Electrochem. Communications*, 7 (2005) 572.
16. C. A. Huang, U. W. Lieu , and C. H. Chuang, *Surf. Coat. Technol.*, 203 (2009) 2921.
17. P. Najafi Sayar and M. Bahrololoom, *Tran. Instit. Met. Finish.*, 87 (2009) 246.
18. H. El Kadi, *Com. Struc.*, 73 (2006) 1.
19. N. Morawej, D. G. Ivey , and S. Akhlaghi Improvements in the Process for Electrodeposition of Au-Sn Alloys. *CS MANTECH Conference, Vancouver, British Columbia, Canada, April*, (2006) 24.
20. Y. B. Song and D. T. Chin, *Electrochim. acta.*, 48 (2002) 349.
21. E. Crabb, E. Moore , and L. Smart *Concepts in Transition Metal Chemistry*: Royal Society of Chemistry,(2009).
22. S. S. Kazhikenova, O. Nurkenov , and B. Satbaev, *Ref. Indust.l Ceram.*, 52 (2011) 55.
23. C. Fontanesi, R. Giovanardi, M. Cannio et al., *J. App. Electrochem.*, 38 (2008) 425.
24. J. Golby and J. Dennis, *Surf. Technol.*, 12 (1981) 141.
25. D. Kim, M. Kim, K. Nam et al., *Surf. Coat. Technol.*, 169 (2003) 650.

26. V. Protsenko, V. Gordiienko, F. Danilov et al., *J. Chem.*, 8 (2011) 1925.
27. V. Gordiienko, F. Danilov , and S. Kwon, *Met. Finishing*, 109 (2011) 33.
28. F. Danilov and V. Protsenko, *Prot. Met.*, 37 (2001) 223.
29. M. Svensson and G. Holmborn Thickness Distribution Control of Electrodeposited Nickel Pads for Microelectronic Interconnections. *Proc. AESF annual tech. conf.* 82, (1995) 145.
30. K. Popov, S. Zecevic, S. Pesic et al., *J. Serbian Chem. Soc.*, 61 (1996) 1225.
31. S. C. Ferreira, R. Bruns, H. Ferreira et al., *Anal. Chim. Acta.*, 597 (2007) 179.
32. C. Madeira, S. Ribeiro, M. Turk et al., *Biotechnol. lett.*, 32 (2010) 1393.
33. M. Paunovic and M. Schlesinger, *Fundamentals of Electrochemical Deposition, Second Edition* (2005).